THE ASTROPHYSICAL JOURNAL, 468:191–198, 1996 September 1

X-RAY EMISSION OF ACTIVE GALACTIC NUCLEI WITH CIRCUMNUCLEAR STAR-FORMING RINGS: NGC 1097 AND NGC 7469

DIEGO E. PÉREZ-OLEA[1,2] AND LUIS COLINA[1,3]
Received 1996 January 18; accepted 1996 March 15

ABSTRACT

ROSAT high-resolution imager (HRI) observations of the active galaxies NGC 1097 (Liner/Seyfert) and NGC 7469 (Seyfert 1), known to have a circumnuclear star-forming ring, are presented. An extended X-ray emission associated with ring of NGC 1097 is detected in the HRI image of this galaxy. The X-ray luminosity emitted by the ring is $L_X = 3.6 \times 10^{40}$ ergs s^{-1} and accounts for about 20% of the integrated X-ray luminosiy of NGC 1097, $L_X = 2 \times 10^{41}$ ergs s^{-1}.

Circumnuclear star-forming rings in active galaxies like NGC 1097 and NGC 1068 have X-rays to radio and Hα luminosities ratios similar to those of pure starburst galaxies like M82, NGC 253, and NGC 1808. On average, starbursts are characterized by $L_X/L_{5\ GHz} \sim 400$, and $L_X/L_{H\alpha} \sim 0.14$.

The HRI image of NGC 7469 shows no structure, and the X-ray emission emitted by the circumnuclear ring cannot be disentangled from that of the nucleus. However, assuming the star-forming ring in NGC 7469 radiates with the average $L_X/L_{5\ GHz} = 400$ of starbursts, a X-ray luminosity $L_X = 5.6 \times 10^{41}$ ergs s^{-1} is inferred. The ring contributes therefore to only about 4% of the integrated X-ray luminosity, $L_X = 1.1 \times 10^{43}$ ergs s^{-1}.

Pure active galactic nuclei (AGNs) are well differentiated from pure starbursts in the $L_X/L_{H\alpha}$ ratio, independent of their absolute luminosity and activity level. For a given Hα luminosity, AGNs produce 100 times more X-rays than pure starbursts do.

The weak X-ray sources detected in some high-luminosity and ultraluminous infrared galaxies are characterized by X-ray to Hα and to radio luminosity ratios $L_X/L_{H\alpha} \sim 0.05$ and $L_X/L_{5\ GHz} \sim 20$, respectively. These values are consistent with the ratios measured in nearly edge-on starbursts but about 100 times smaller than those of composite AGNs plus circumnuclear star-forming galaxies like NGC 1097 and NGC 7469.

Subject headings: galaxies: active — galaxies: individual (NGC 1097, NGC 7469) — galaxies: Seyfert — galaxies: starburst — galaxies: structure — X-rays: galaxies

1. INTRODUCTION

Circumnuclear star-forming rings have been found in several active galaxies with different types of activity ranging from starbursts (NGC 3351, NGC 3504), to low-luminosity active galactic nuclei (NGC 1097) and Seyfert galaxies (NGC 1068, NGC 7469). Also, high-luminosity and ultraluminous infrared galaxies are places in which an active galactic nucleus (AGN) seems to coexist with circumnuclear starbursts (Krabbe & Colina 1996; Veilleux et al. 1995; Colina & Pérez-Olea 1992). In some of these active galaxies, the AGN is not the dominant energy source at infrared, optical, or ultraviolet wavelengths. Prototypical examples are the nearby Seyfert 2 galaxy NGC 1068 and the high-luminosity Seyfert 1 galaxy NGC 7469, in which the nuclear and circumnuclear star-forming regions dominate the ultraviolet (Neff et al. 1994) and infrared (Genzel et al. 1995) energy output, respectively.

Star-forming regions are also sources of X-ray emission generated by X-ray binaries, young supernovae, and supernova remnants. What is the contribution of circumnuclear star-forming regions to the X-ray energy output in composite AGN plus starburst galaxies? Studies on the fractional contribution of nuclear/circumnuclear star-forming rings in active galaxies are very scarce, as *ROSAT*/HRI spatial resolution (FWHM ~ 5″) is only good enough to separate the AGN from the star-forming component in nearby face-on galaxies. So far, the fractional AGN/starburst X-ray contribution has been studied only in NGC 1068 (Wilson et al. 1992). These authors conclude that 22% of the soft X-ray emission originates in the star-forming ring, while another 23% is an extended nuclear component. New HRI observations of nearby face-on circumnuclear star-forming galaxies are needed to characterize the X-ray properties of starbursts.

On the other hand, ultraluminous infrared galaxies (ULIRGs) classified as Seyfert galaxies (Veilleux et al. 1995) have not yet been detected in hard (2–10 keV) X-rays (Rieke 1988). ULIRGs are therefore underluminous in X-rays relative to optically selected AGNs by factors 6–600 (Rieke 1988). Recent infrared observations of Mrk 231 (Krabbe & Colina 1996) indicate that the nucleus of this ultraluminous infrared galaxy should be transparent to hard X-ray radiation. These results suggest that ULIRGs are not powered by an embedded X-ray–bright quasar but by either a low-luminosity X-ray quasar or an intense nuclear and circumnuclear star formation process, or a combination of both. By investigating the X-ray properties of nearby well-resolved composite AGN plus starburst galaxies and comparing these results with those obtained for ULIRGs, some insight into the source of X-rays in luminous infrared galaxies can be inferred.

New observations with the *ROSAT* HRI of two galaxies with known circumnuclear star-forming rings, NGC 1097 ($D = 17$ Mpc, using $H_0 = 75$ km s^{-1} Mpc^{-1} hereafter) and

[1] Space Telescope Science Institute, 3700 San Martin Drive, Baltimore, MD 21218.
[2] Dpto. de Física Teórica C-XI, Universidad Autónoma de Madrid, 28049 Madrid, Spain; perez@stsci.edu.
[3] On assignment from the Space Science Department of ESA.

NGC 7469 ($D = 65.5$ Mpc) are presented in this paper. The angular resolution of the HRI (FWHM $\sim 5''$) allows us to separate the two components (AGN and star-forming ring) for NGC 1097 and measure the integrated luminosity in NGC 7469. The nuclear ring in NGC 1097 is located at a radius of 0.8 kpc ($\sim 10''$) from the nucleus, which is classified as a low-ionization nuclear emission-line region (LINER) (Keel 1983; Phillips et al. 1984), although it has recently shown a variable double peak broad Hα line in emission (Storchi-Bergmann, Baldwin, & Wilson 1993; Storchi-Bergmann et al. 1995). The nuclear ring has been studied in detail in Hα and at 5 GHz (Hummel, van der Hulst, & Keel 1987, hereafter HHK87).

The high-luminosity Seyfert 1 galaxy NGC 7469 has a circumnuclear ring at a radius of about 0.48 kpc ($1''.5$; Wilson et al. 1991) that dominates the bolometric luminosity (Genzel et al. 1995). NGC 7469 has been studied exhaustively at different wavelengths with high spatial resolution (radio, Wilson et al. 1991; molecular, Meixner et al. 1990; infrared, Genzel et al. 1995; optical, Wilson et al. 1986; Mauder et al. 1994).

In § 2 the new *ROSAT* HRI observations of NGC 1097 and NGC 7469 as well as the data analysis are presented, while the results are explained in § 3. Section 4 focuses on a discussion of the contribution of circumnuclear starbursts to the X-ray energy output in different types of active galaxies, including luminous galaxies.

2. OBSERVATIONS AND DATA ANALYSIS

NGC 7469 was observed with the *ROSAT* high-resolution imager (HRI) in 1993 June 15 and 1994 May 30, for an integration time of 4088 s, divided into four independent images (OBIs). The final image is created by coadding the individual OBIs after recentering to the position of the peak intensity. NGC 1097 was observed over the period 1994 July 11–12 for an integration time of 8837 s. As in the previous case, the individual OBIs were recentered and co-added. Analysis of the images was performed using the PROS package under IRAF. For NGC 7469, the final image was obtained using a blocking factor of 1 in the co-added image and smoothing it with a $3''$ FWHM Gaussian filter. In the same way, the final HRI image of NGC 1097 is obtained using a blocking factor of 2 and a $5''$ FWHM Gaussian filter.

The background levels for NGC 7469 and NGC 1097, as measured in one annulus centered in the nucleus with radii $3'$ and $8'$, are 1.66×10^{-6} counts s^{-1} arcsec^{-1} and 1.09×10^{-6} counts s^{-1} arcsec^{-1}, respectively.

The count rates for NGC 7469 and NGC 1097 are given in Table 1. To transform the corresponding count rates into flux in the HRI 0.1–2.4 keV band, the procedure outlined in David et al. (1995) has been followed. Since the energy to count conversion factors (ECFs; David et al. 1995) depend on the radiation mechanism (power-law, blackbody, bremsstrahlung) and on the internal extinction, the parameters characterizing the radiation mechanism and the amount of extinction have to be established independently for NGC 7469 and NGC 1097.

2.1. *Flux Calibration of NGC 7469 ROSAT/HRI Image*

The ECF conversion factor for NGC 7469 is obtained by assuming that NGC 7469 has an X-ray spectrum characterizied by a power law of photon index $\Gamma = 2.26 \pm 0.05$ and a column density of $N_{\rm H} = (5.7 \pm 0.2) \times 10^{20}$ cm^{-2} (Brandt et al. 1993). For comparison, the corresponding galactic column density is $N_{\rm H}^{\rm gal} = (4.83 \pm 0.72) \times 10^{20}$ cm^{-2} (Elvis, Lockman, & Wilkes 1989).

2.2. *Flux Calibration of NGC 1097 ROSAT/HRI Image*

For NGC 1097, different radiation mechanisms and extinctions have to be considered for the nucleus and circumnuclear starburst.

The nucleus of NGC 1097 is classified as a LINER, based on the optical spectra (Keel 1983; Phillips et al. 1984), although Storchi-Bergmann et al. (1993, 1995) have recently reported the detection of a variable broad Hα emission line, typical of Seyfert 1 galaxies. To determine the parameters characterizing the X-ray emission of the NGC 1097 nucleus, X-ray observations of LINERs are used. *ROSAT* PSPC spectra of some LINERs are best fitted by a power-law spectra, with an average photon index $\Gamma \approx 2.8$ (NGC 3642: $\Gamma = 2.84 \pm 0.67$, NGC 4278: $\Gamma = 2.76 \pm 1.15$, Koratkar et al. 1995). However, in NGC 4258 the power law is steeper ($\Gamma = 3.7$; Pietsch et al. 1994) and for M81 there is no agreement in the results. While *Einstein* IPC observations are best fitted by a power law with photon index $\Gamma = 4^{+2}_{-1.5}$ (Fabbiano 1988a), BBXRT and *ROSAT* PSPC spectra agree with a power law with photon indexes $\Gamma = 2.2$ and $\Gamma = 2.0$, respectively (Petre et al. 1993). Therefore, for the X-ray spectrum of the NGC 1097 nucleus, a power law with a photon index equal to the average of all the above-mentioned observations, i.e., $\Gamma = 3$, is assumed here.

Using the Balmer decrement, Storchi-Bergmann et al. (1993) measured a high extinction toward the nucleus, equivalent to $E(B-V) \geq 0.73$. A column density $N_{\rm H} \geq 4.2 \times 10^{21}$ cm^{-2} is obtained using the expression $N({\rm H\ I} + H_2) = 5.8 \times 10^{21} \times E(B-V)$ cm^{-2} (Bohlin, Savage, & Drake 1978). For comparison, the galactic column density is only $N_{\rm H}^{\rm gal} = 1.9 \times 10^{20}$ (Kim, Fabbiano, & Trinchieri 1992).

To determine the parameters characterizing the X-ray emission in the star-forming ring of NGC 1097, *Einstein* and *ROSAT* observations of nearby starburst galaxies are used. Fabbiano (1988b) fitted the *Einstein* IPC spectra of M82 and NGC 253 using a plasma radiating at temperatures $kT \sim 1.2$ and 2.2 keV, respectively. The X-ray spectrum of NGC 6946 fits with a temperature $kT = 0.8$ keV (Fabbiano & Trinchieri 1987), while *ROSAT* PSPC spectra of other

TABLE 1

HRI OBSERVATIONS OF NGC 1097 AND NGC 7469

Galaxy	$t_{\rm exp}$ (s)	Background (counts s^{-1} arcsec^{-1})	Aperture (arcsec)	Count Rate (10^{-2})
NGC 7469.....	4088	1.66×10^{-6}	5×5	12.6 ± 0.6
NGC 1097.....	8838	1.09×10^{-6}	5×5	0.36 ± 0.08
			6–14	0.74 ± 0.08[a]

[a] Scattered counts from the nucleus have been removed.

starburst galaxies are fitted with even lower values of kT (NGC 1808: $kT = 0.5$ keV, Junkes et al. 1995; NGC 3077; $kT = 0.65$ keV, Bi, Arp, & Zimmermann 1994). Therefore, a plasma with a temperature $kT = 1$ keV is used here to characterize the X-ray emission generated by the circumnuclear ring of NGC 1097.

As for the nucleus, the internal extinction in the circumnuclear ring of NGC 1097 is derived from the Balmer decrement, measuring an extinction equivalent to $E(B-V) = 0.3$–0.9 in different regions (HHK87). An intermediate value $E(B-V) = 0.6$ is considered here for the whole ring. Using the standard $E(B-V)$ to N_H conversion factor (Bohlin et al. 1978), a column density of $N_H = 3.5 \times 10^{21}$ cm^{-2} is derived, a factor about 20 larger than the galactic one.

3. RESULTS

3.1. *NGC 7469*

The circumnuclear star-forming ring in NGC 7469 is located at a radius about 1.″5 of the nucleus (Wilson et al. 1991; Genzel et al. 1995), which is significantly smaller than the *ROSAT* HRI resolution. NGC 7469 does not show any evidence for extended X-ray emission in the HRI image (Fig. 1). The elongation in the northwest direction may be due to the HRI point-spread function (PSF) itself, as *ROSAT* HRI images of X-ray point sources show a similar asymmetry (Morse 1994).

The azimuthal profile for NGC7469 (Fig. 2) fits to a Gaussian of FWHM $\sim$ 6.″2, wider than the theoretical PSF

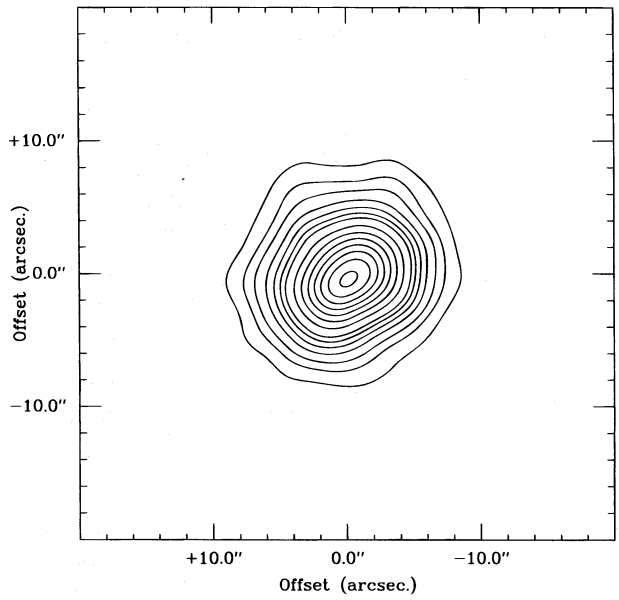

FIG. 1.—Contour map for the X-ray emission in NGC 7469. Contour levels are 2.5, 5, 10, 15, 20, 25, 30, 40, 50, 60, 70, 80, 90, and 100% of the peak intensity, 32 counts arcsec^{-1}.

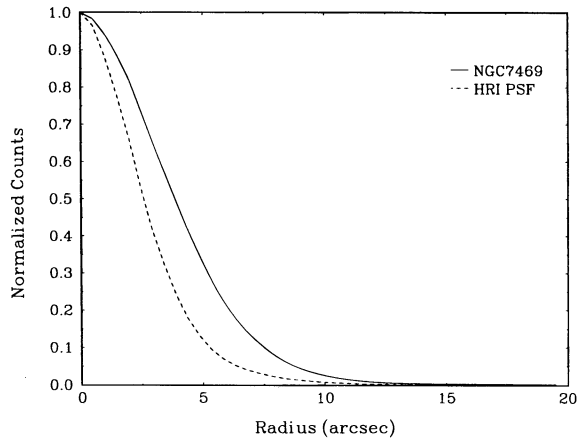

FIG. 2.—Radial profile for NGC 7469 (*solid line*) and the theoretical HRI PSF (*dashed line*).

of the HRI (FWHM $\sim$ 5.″2). The errors in pointing ($\sim$0.″5) and in the recentering process ($\sim$0.″5) together with the Gaussian filter used, with FWHM $\sim$ 3″, account for the difference between the theoretical and measured FWHM of the PSF (the theoretical profile is also plotted for reference in Fig. 2).

The derived flux and luminosity for the extinction and power-law photon index discussed above (see § 2.1) are given in Table 2. The integrated 0.1–2.4 keV X-ray luminosity of NGC 7469 corresponds to $L_X = 1.1 \times 10^{43}$ ergs s^{-1}, in agreement with Brandt et al. (1993) results, and about 60% lower than the luminosity measured by Turner, George, & Mushotzky (1993).

3.2. *NGC 1097*

The structure of the X-ray emission in the central 40″ region of NGC 1097 is shown in Figure 3. Besides the emission from the nucleus, there is extended emission spatially coincident with the circumnuclear star-forming ring, as shown in the Hα and radio contour maps of NGC 1097 (taken from HHK87) overlaid to the gray-scaled X-ray image (Figs. 4*a* and 4*b*). The peak of the X-ray emission is coincident with the optical nucleus of the galaxy, while low surface brightness X-ray emission extends beyond the Hα ring.

The derived fluxes and luminosities for the nucleus and circumnuclear star-forming ring are listed in Table 2. The 0.1–2.4 keV X-ray luminosity for the nuclear source is $L_X = 1.64 \times 10^{41}$ ergs s^{-1}. This luminosity is a factor of 10 higher than the soft X-ray luminosities measured in other LINERs (NGC 3642 and NGC 4278: $\sim 1.7 \times 10^{40}$ ergs s^{-1}, Koratkar et al. 1995; M81: 9×10^{39} ergs s^{-1}, Fabbiano, Kim, & Trinchieri 1992). It could well be that the NGC 1097 nucleus was under a high activity phase at the time of

TABLE 2

HRI FLUX AND LUMINOSITIES OF NGC 1097 AND NGC 7469

Galaxy	N_H (10^{20} cm^{-2})	Γ	kT (keV)	f_X(0.1–2.4 keV) (10^{-12} ergs cm^{-2} s^{-1})	L_X(0.1–2.4 keV) (10^{41} ergs s^{-1})
NGC 7469.....	5.72	2.26	...	21.0 ± 1.0	108 ± 5
NGC 1097 (nucleus).....	42.2	3.0	...	4.75 ± 1.10	1.64 ± 0.36
NGC 1097 (ring).....	34.8	...	1.0	1.03 ± 0.11	0.36 ± 0.04

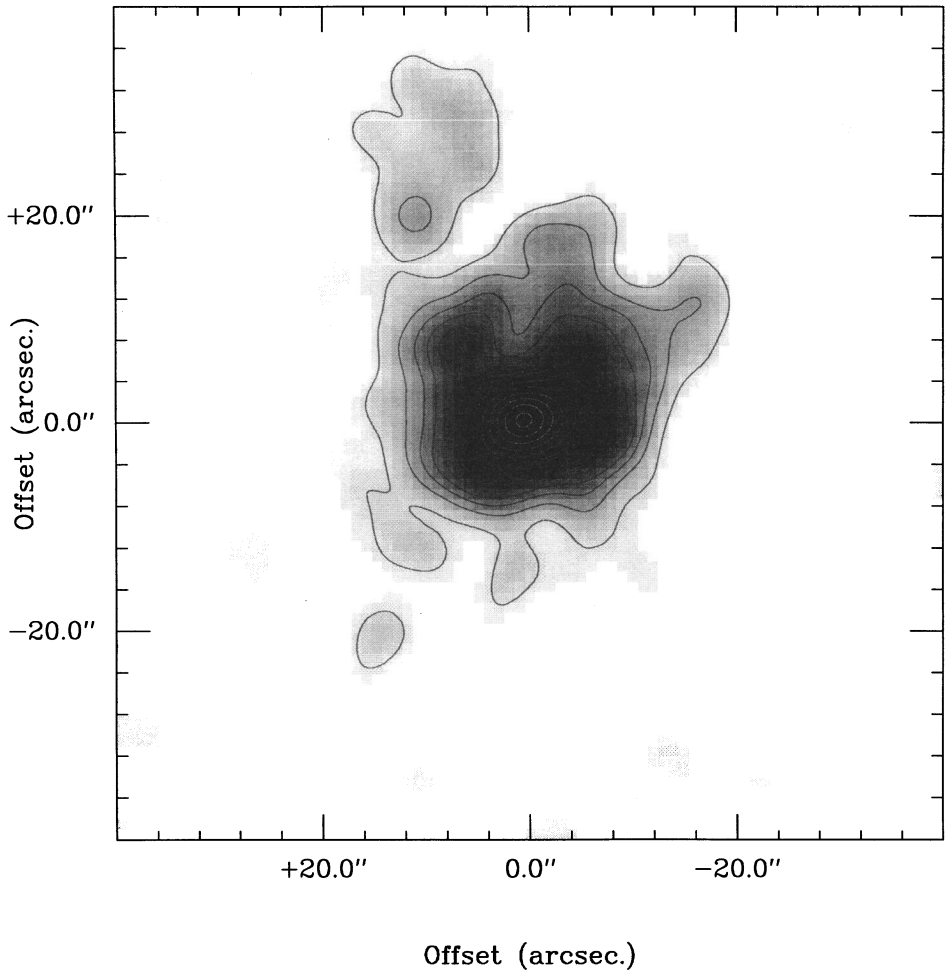

FIG. 3.—Gray-scaled map for the X-ray emisson in NGC 1097. Contours are also displayed to enhance the structure. Contour levels are 5, 10, 15, 20, 25, 30, 35, 40, 50, 60, 70, 80, 90, and 100% of the peak intensity, 1.49 counts arcsec^{-1}.

the *ROSAT* observations, as optical observations suggest by the presence of a variable broad Hα line in emission (Storchi-Bergmann et al. 1993, 1995).

The circumnuclear star-forming ring in NGC 1097 extends between 5″ and 15″ from the nucleus (∼0.4–1.2 kpc) as traced by the Hα and radio images. The contribution of the circumnuclear star-forming ring to the total X-ray luminosity is seen more clearly in Figure 5, where the X-ray

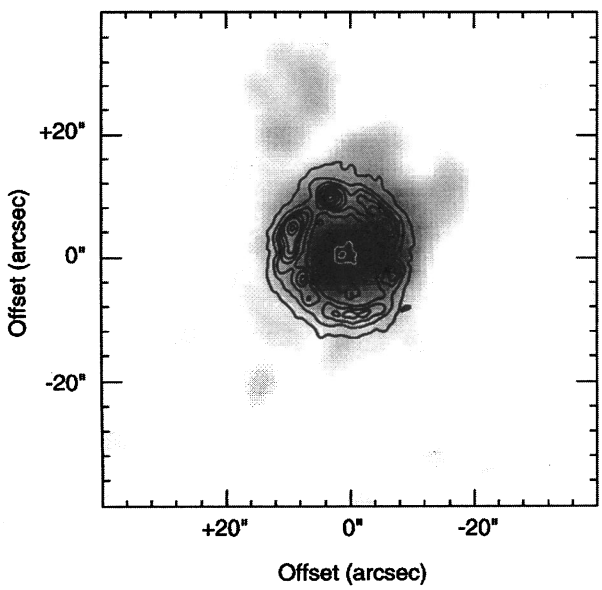

FIG. 4*a*

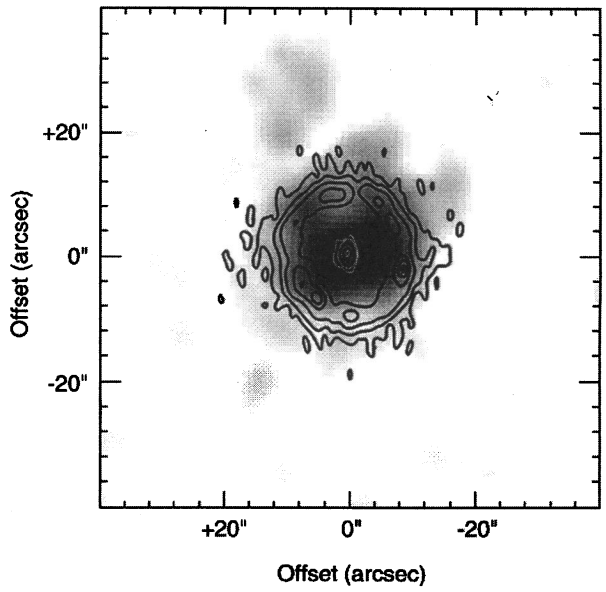

FIG. 4*b*

FIG. 4.—(*a*) Hα contour map for NGC 1097 superimposed over the gray-scaled X-ray image. (*b*) 5 GHz radio map superimposed over the gray-scaled X-ray image. Both Hα and radio contour maps are from Hummel et al. (1987). Some contours in the Hα and radio map have been removed for clarity.

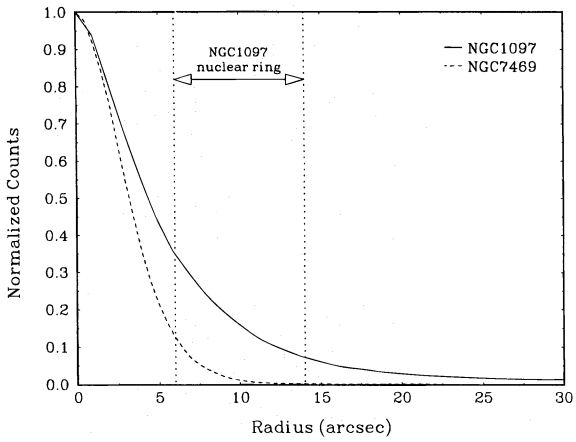

FIG. 5.—Radial profile for NGC 1097 (*solid line*) and NGC 7469 (*dashed line*). The extent of the circumnuclear region in NGC 1097 is shown.

radial profile of NGC 1097 and the region in which the circumnuclear ring extends are plotted. The total 0.1–2.4 keV X-ray luminosity derived for the ring is 3.6×10^{40} ergs s^{-1} (see Table 2).

The integrated 0.1–2.4 keV X-ray luminosity emitted by NGC 1097 is therefore 2.0×10^{41} ergs s^{-1}, where the circumnuclear star-forming ring contributes about 20%. The fractional contribution of the star-forming ring to the integrated X-ray luminosity depends heavily on the true temperature of the radiating plasma associated with the starburst, and in particular on the true photon index of the nonthermal emission emitted by the nucleus. The circumnuclear star-forming ring could contribute as much as 50% of the total X-ray luminosity if the nucleus emits with a photon-index $\Gamma \sim 1.5$.

4. DISCUSSION

Besides NGC 1097 and NGC 7469, NGC 1068 has been observed with the *ROSAT* HRI (Wilson et al. 1992). These three active galaxies are known to have star-forming circumnuclear rings while covering a wide range in the AGN activity scale from low luminosity (NGC 1097) to Seyfert 2 (NGC 1068) and luminous Seyfert 1 (NGC 7469). The X-ray energy output of these three galaxies can then be compared to study, as a function of luminosity, the contribution of circumnuclear star-forming rings to the total X-ray luminosity emitted by composite AGN plus star-forming galaxies. The X-ray luminosity for a sample of nearby AGNs and pure starbursts for which *ROSAT* or *Einstein* HRI data are available in the literature is also included for comparison (L_X in Table 3). Other properties like the radio luminosity at 5 GHz, computed as $\nu \times L_\nu$ ($L_{5\,\mathrm{GHz}}$ in Table 3 and hereafter), and the Hα luminosity ($L_{H\alpha}$ in Table 3) are also indicated for the sample. To minimize extinction effects, Hα luminosities are derived from Brγ luminosities when available, using $\mathrm{Br}\gamma/\mathrm{H}\alpha = 0.01$. When Hα flux is used, a correction for internal extinction has been made if $E(B-V)$ is known.

4.1. *Circumnuclear Star-forming Rings*

The circumnuclear star-forming rings in NGC 1097 and NGC 1068 (indicated as SB in Table 3) display the same range of X-ray luminosities, $L_X/L_{5\,\mathrm{GHz}}$ and $L_X/L_{H\alpha}$ ratios as those observed in nearby starburst galaxies like M82, NGC 253, and NGC 1808 (Table 3). These circumnuclear star-forming rings and starbursts are characterizied by X-ray luminosities (L_X) in the 7×10^{38} ergs s^{-1} to 1×10^{41} ergs s^{-1} range, and luminosity ratios $L_X/L_{5\,\mathrm{GHz}} \sim 15$–$10^3$ and $L_X/L_{H\alpha} \sim 0.03$–$0.3$ (Table 3 and Fig. 6b). On average, starbursts can be characterized by X-ray to radio and Hα luminosity ratios $L_X/L_{5\,\mathrm{GHz}} \sim 400$ and $L_X/L_{H\alpha} \sim 0.14$.

X-ray luminosity in starbursts arises from supernovae explosions, supernova remnants, and X-ray binary systems. Some Type II supernovae are strong X-ray sources with luminosities $L_X \sim 10^{38}$–10^{40} ergs s^{-1} (SN 1978k: Ryder et al. 1993, Colbert et al. 1995; SN 1986J: Bregman & Pildis 1992; SN 1993J: Schlegel 1994). X-ray binaries produce typical X-ray luminosities $\sim 10^{36}$–10^{38} ergs s^{-1}, while galactic supernova remnants have luminosities in the 10^{33}–10^{39} ergs s^{-1} range. Thus, a combination of X-ray binaries,

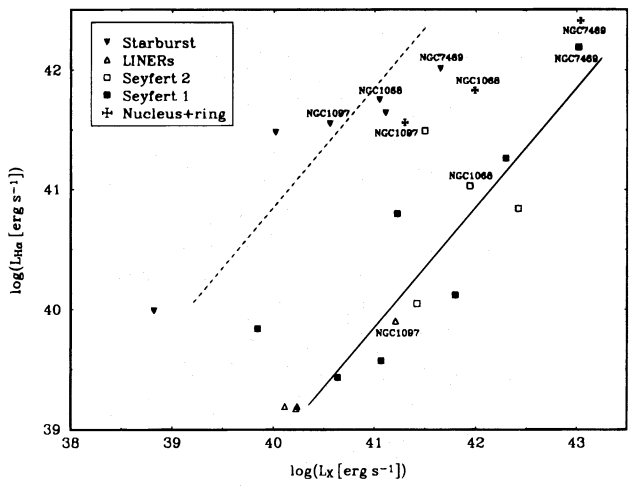

FIG. 6*a*

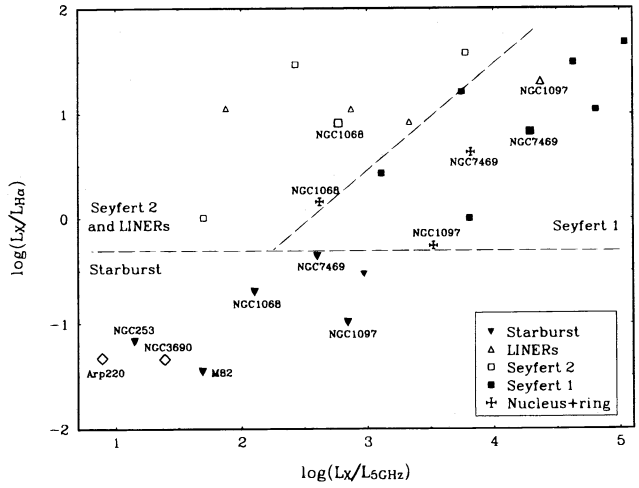

FIG. 6*b*

FIG. 6.—(*a*) Relation between X-ray and the Hα luminosities for starbursts and AGNs. The position of the circumnuclear starbursts, nuclei, and integrated values for NGC 1068, NGC 1097, and NGC 7469 are indicated. The correlation found by Ward 1988 (*dashed line*) and Koratkar et al. 1995 (*solid line*) are also plotted. (*b*) Diagram log ($L_X/L_{H\alpha}$) vs. log ($L_X/L_{5\,\mathrm{GHz}}$) for starbursts, luminous infrared galaxies, and AGNs. The position of the circumnuclear starbursts, nuclei, and integrated values for NGC 1068, NGC 1097, and NGC 7469 are also indicated. Note that different types of active galaxies are distributed in different locations, separated by the dashed line.

TABLE 3

X-RAY, RADIO, AND Hα LUMINOSITIES OF ACTIVE GALAXIES

Galaxy	D (Mpc)	Type	log (L_X) (ergs s^{-1})	log ($L_{5\,GHz}$) (ergs s^{-1})	log ($L_{H\alpha}$) (ergs s^{-1})	log ($L_X/L_{5\,GHz}$)	log ($L_X/L_{H\alpha}$)	Reference
NGC 1068.....	15.0	SB	41.05[a]	38.95	41.75	2.10	−0.70	1, 2, 3, 4
	15.0	Sy2	41.94	39.17	41.03[b]	2.77	+0.91	1, 5, 6
	15.0	Sy2 + SB	41.99	39.37	41.83	2.62	+0.16	
NGC 1097.....	17.0	SB	40.56	37.72	41.55	2.84	−0.99	7, 8
	17.0	LINER	41.21	36.85	39.90	4.37	+1.31	7, 8, 9
	17.0	LINER+SB	41.30	37.78	41.56	3.52	−0.26	
NGC 7469.....	65.5	SB	(41.65)[c]	39.05	42.01[b]	(2.60)	(−0.36)	7, 10, 11
	65.5	Sy1	(43.02)[c]	38.73	42.19[b]	(4.29)	(+0.83)	7, 10, 11
	65.5	Sy1 + SB	43.04	39.22	42.41	3.82	+0.63	
M82	3.25	SB	40.02[d]	38.33	41.48[b]	1.69	−1.46	12, 13, 14
NGC 253	2.5	SB	38.82[d]	37.67	39.99[b]	1.15	−1.17	13, 14, 15, 16
NGC 1808.....	10.9	SB	41.11	38.14[e]	41.64[b]	2.97	−0.53	17, 18, 19
M81	3.3	LINER	40.11[f]	36.78	39.19	3.33	+0.92	20, 21, 22
NGC 3642.....	21.2	LINER	40.24	37.37[e]	39.19	2.87	+1.05	23, 24
NGC 4278.....	8.7	LINER	40.22	38.34	39.17	1.88	+1.05	23, 25
Mrk 3.....	54.0	Sy2	41.50	39.80	41.49	1.70	+0.01	26, 27, 28
NGC 2110.....	30.5	Sy2	41.42	38.99	40.05	2.43	+1.47	5, 29, 30
NGC 2992.....	30.9	Sy2	42.42[f]	38.64	40.84	3.78	+1.58	5, 20, 31
NGC 3516.....	34.7	Sy1	42.30	37.49	41.26	4.81	+1.04	5, 26, 32
NGC 4151.....	13.3	Sy1	41.23	38.12	40.80[b]	3.11	+0.43	5, 26, 31
NGC 4639.....	13.5	Sy1	40.64	36.89[g]	39.43	3.75	+1.21	23, 33
NGC 5033.....	11.7	Sy1	41.06	36.43	39.57	4.63	+1.49	23, 34
NGC 5273.....	14.1	Sy1	39.84	36.03	39.84	3.81	+0.00	5, 23
NGC 6814.....	20.8	Syl	41.80[f]	36.76	40.12	5.04	+1.68	5, 20, 35

[a] Using $kT = 1$ keV and $N_H = 3 \times 10^{20}$ cm^{-2}.
[b] Derived from Brγ.
[c] Estimated. See § 4.1.
[d] From *Einstein* HRI observations, with spectral parameters given in Fabbiano & Trinchieri 1984.
[e] Derived from 20 cm observations assuming a spectral index $\alpha = 0.65$ (NGC 1808) and $\alpha = 0.7$ (NGC 3642).
[f] From *Einstein* HRI observations assuming a power law with $\Gamma = 3$.
[g] Derived from 2.8 cm observations assuming a spectral index $\alpha = 0.7$.

REFERENCE.—(1) Wilson et al. 1992. (2) Condon et al. 1982. (3) Bland-Hawthorn, Sokolowsky, & Cecil 1991. (4) Bruhweiler, Truong, & Attner 1991. (5) Ulvestad & Wilson 1984b. (6) Rotaciuc et al. 1991. (7) This work. (8) HHK87. (9) Storchi-Bergmann et al. 1993. (10) Wilson et al. 1991. (11) Genzel et al. 1995. (12) Watson, Stanger, & Griffiths 1984. (13) Fabbiano & Trinchieri 1984. (14) Ho, Beck, & Turner 1990. (15) Fabbiano 1988b. (16) Forbes et al. 1993. (17) Dahlem, Hartner, & Junkes 1994. (18) Saikia et al. 1990. (19) Krabbe, Sternberg, & Genzel 1994. (20) Fabbiano et al. 1992. (21) Turner & Ho 1994. (22) Filippenko & Sargent 1988. (23) Koratkar et al. 1995. (24) Hummel 1985. (25) Wrobel 1991. (26) Morse et al. 1995. (27) Ulvestad & Wilson 1984a. (28) Miller & Goodrich 1990. (29) Weaver et al. 1995. (30) Schuder 1980. (31) Forbes & Ward 1993. (32) Kim 1989. (33) Niklas, Klein, & Wielebinski 1995. (34) Ulvestad & Wilson 1989. (35) Schulz, Knake, & Schmidt-Kaler 1994.

young supernovae, and supernovae remnants can easily produce the observed X-ray luminosities in the 10^{39}–10^{41} ergs s^{-1} range.

The range of values displayed by the $L_X/L_{5\,GHz}$ ratio can most likely be explained in terms of absorption of X-rays by the dense and dusty interstellar environment present in starbursts. As we move from face-on (NGC 1068, NGC 1097) to edge-on (M82, NGC 253) starbursts, X-rays will get absorbed very efficiently by the dense medium, while the radio emission will still be transparent. Thus, M82 or NGC 253 starbursts have the lowest $L_X/L_{5\,GHz}$, while the NGC 1097 ring has one of the highest $L_X/L_{5\,GHz}$ ratios (see Table 3).

The X-ray luminosity has a strong linear correlation with the $L_{H\alpha}$ luminosity and agrees with the $L_X = 14 \times L_{Br\gamma}$ ratio found by Ward (1988) for a sample of starburst galaxies, if the Hα to Brγ case B recombination value is adopted (dashed line in Fig. 6*a*).

In our *ROSAT*/HRI image of NGC 7469, the X-ray emission associated with the circumnuclear star-forming ring cannot be disentangled from the emission coming from the nucleus. However, an estimation of the soft X-ray luminosity emitted by the ring can be inferred using the average X-ray to radio luminosity ratio of starbursts ($L_X/L_{5\,GHz} \sim 400$). If $L_{5\,GHz}^{ring} = 1.1 \times 10^{39}$ ergs s^{-1} (see Table 3 and references), the X-ray luminosity produced in the ring will be $L_X^{ring} \sim 4.4 \times 10^{41}$ ergs s^{-1}. Compared to the integrated X-ray luminosity of NGC 7469, $L_X = 1.1 \times 10^{43}$ ergs s^{-1}, the contribution from the star-forming ring is only 4%. Thus, even if the bolometric luminosity of NGC 7469 is dominated by the energy output from the circumnuclear ring (Genzel et al. 1995), its X-ray luminosity represents only a rather small fraction of that of the nucleus.

Thus, as we move from NGC 1097 to NGC 1068 and NGC 7469, i.e., toward higher X-ray luminosities in composite AGNs plus star-forming galaxies, the contribution of the circumnuclear star-forming ring to the integrated X-ray luminosity decreases from about 20% to 10%, and 4% (see values in Table 3). It could well be, as discussed in § 3.2, that star-forming rings can contribute with an even larger fraction (∼50%) of the total X-ray luminosity in low-luminosity galaxies like NGC 1097, but it is hard for star-forming galaxies to produce very luminous soft X-ray sources, i.e., $L_X \geq 5 \times 10^{41}$ ergs s^{-1}, as the median soft X-ray to far-infrared luminosity ratio of bright infrared galaxies is $L_X/L_{FIR} = 10^{-3.4}$ (David, Jones, & Forman 1992).

4.2. *Active Galactic Nuclei*

Pure AGNs covering the same range in X-ray luminosities as nearby starbursts are differentiated from pure starbursts in the $L_X/L_{5\,GHz}$ versus $L_X/L_{H\alpha}$ diagram (see Fig. 6*b* and Table 3). Liners and some Seyfert 2 galaxies have an

$L_X/L_{5\ GHz}$ ratio similar to that observed in starburst galaxies like NGC 1808 or circumnuclear star-forming rings like in NGC 1097. Seyfert 1 galaxies have on average a X-ray to radio luminosity ratio 100 times that observed in starbursts (see Fig. 6*b* and Table 3). Mas-Hesse et al. (1994) have also recently found two orders of magnitude difference in the $L_{soft-X}/L_{60\ \mu m}$ ratio between Seyfert 1 galaxies and starbursts.

The larger difference between pure AGNs and pure starbursts or circumnuclear star-forming rings appears, however, in the $L_X/L_{H\alpha}$ ratio. For a given Hα luminosity, AGNs are 100 times more powerful than starbursts in X-rays (see Table 3). Also, pure AGNs covering 3 orders of magnitude in X-ray luminosity follow a correlation between soft X-rays and Hα similar to the one found by Koratkar et al. (1995) for a sample of low-luminosity active galaxies, for which $L_X = 14 \times L_{H\alpha}$ (solid line in Fig. 6*a*).

4.3. *Composite AGN plus Starbursts and the Origin of X-Rays in Luminous Infrared Galaxies*

Most high-luminosity and ultraluminous infrared galaxies (ULIRGs) are classified as LINERS or Seyfert 2 galaxies, based on the optical emission-line ratios (Veilleux et al. 1995). However, evidence for the presence of nuclear or circumnuclear starbursts in these galaxies exists also (Condon et al. 1991; Heckman, Armus, & Miley 1990). Moreover, detection of ULIRGs has failed at hard X-ray bands (Rieke 1988), placing a limit to the hard 2–10 keV X-ray luminosity of $L_{HX} < 10^{-2.7} \times L_{FIR}$, while recent infrared observations of the ultraluminous infrared Seyfert 1 galaxy Mrk 231 (Krabbe & Colina 1996) suggest that the nucleus of this galaxy should be transparent to the hard X-rays. These observational results favor, as first suggested by Rieke (1988), the presence of a weak X-ray quasar in the center of ULIRGs or the existence of an intense star formation in the nuclear and circumnuclear regions dominating the energy output. Could the luminous infrared galaxies be the more distant analogs of NGC 1097, NGC 1068, or NGC 7469? If so, could the starburst be the dominant X-ray energy sources in these galaxies?

Two high-luminosity infrared galaxies, NGC 3690 (Fabbiano et al 1992) and Arp 220 (Eales & Arnaud 1988; Heckman et al. 1996), have been detected in soft X-rays. With the *Einstein* HRI, Fabbiano et al. (1992) found for NGC 3690 ($D = 48$ Mpc) a total soft X-ray luminosity $L_X = 1.0 \times 10^{41}$ ergs s^{-1}, assuming a Raymond-Smith emission model with $kT \sim 1$ keV. Recently, Heckman et al. (1996) have published new *ROSAT* HRI images for Arp 220 ($D = 78$ Mpc) and derived a luminosity $L_X = 5.1 \times 10^{40}$ ergs s^{-1} using a Raymond-Smith emission model with $kT \sim 0.9$ keV, according to their PSPC spectra. An $L_X/L_{FIR} \sim 10^{-4.5}$ is obtained for these two galaxies considering a FIR luminosity log $L_{FIR} = 11.74\ L_\odot$ and $12.11\ L_\odot$ for NGC 3690 and Arp 220, respectively (Condon et al. 1991). The ultraluminous infrared and Seyfert 1 galaxy Mrk 231 has an upper limit $L_X/L_{FIR} < 10^{-3.8}$ (Eales & Arnaud 1988).

These L_X/L_{FIR} values are even smaller than the expected average ratio for starbursts, but consistent with the ratio observed in nearly edge-on starbursts. Considering the average $L_X/L_{5\ GHz}$ of 400 for starbursts and $L_{5\ GHz}/L_{FIR}$ of $10^{-5.9}$ (Colina & Pérez-Olea 1995), the expected soft X-ray to far-infrared luminosity emitted by starbursts would be $L_X/L_{FIR} \sim 10^{-3.3}$, which agrees with the median $L_X/L_{FIR} \sim 10^{-3.4}$ ratio found by David et al. (1992) for a sample of bright infrared galaxies. For the nearly edge-on starbursts M82 and NGC 253, $L_X/L_{FIR} \sim 10^{-3.7}$, on average (Eales & Arnaud 1988). For comparison, our composite AGN plus circumnuclear star-forming galaxies NGC 1097 and NGC 7469 have a ratio L_X/L_{FIR} equal to $10^{-2.7}$ and $10^{-2.0}$, respectively.

Condon et al. (1991) give the radio flux emitted by NGC 3690 and Arp 220 at 1.49 GHz with 1".5 resolution. Using the radio spectral index $\alpha(6, 20) \sim -0.67$ and $\alpha(6, 20) \sim -0.41$ for each galaxy (Condon et al. 1991), the derived radio luminosity at 5 GHz is $L_{5\ GHz} = 4.05 \times 10^{39}$ ergs s^{-1} and $L_{5\ GHz} = 6.69 \times 10^{39}$ ergs s^{-1}, for NGC 3690 and Arp 220, respectively. The ratio $L_X/L_{5\ GHz}$ of about 20 found in these two luminous infrared galaxies is lower than the average value for starburst galaxies ($\sim$400; see § 4.1) but consistent with that of nearly edge-on starbursts like M82 and NGC 253, in which an average ratio $L_X/L_{5\ GHz} \sim 32$ is measured (see Table 3). For comparison, the integrated (i.e., AGN plus star-forming ring) $L_X/L_{5\ GHz}$ ratios in NGC 1097 and NGC 7469 are 3.3×10^3 and 6.6×10^3, respectively.

Hα luminosities for NGC 3690 and Arp 220 have been obtained from Brγ fluxes given by Doherty et al. (1995) and Goldader et al. (1995) . The derived Hα luminosities correspond to $L(H\alpha) = 2.2 \times 10^{42}$ ergs s^{-1} and $L(H\alpha) = 1.1 \times 10^{42}$ ergs s^{-1} for NGC 3690 and Arp 220, respectively. A ratio $L_X/L_{H\alpha} \sim 0.05$ is found for both galaxies, similar to the ratio found for starbursts such as M82 and NGC 253, and two orders of magnitude smaller than those measured in Seyfert and Liner galaxies (see Fig. 6*b*).

Summarizing, the $L_X/L_{5\ GHz}$, $L_X/L_{H\alpha}$, and L_X/L_{FIR} ratios measured in some high-luminosity and ultraluminous infrared galaxies are consistent with the values measured in nearby edge-on starbursts and inconsistent with the relations observed in composite AGN plus star-forming ring galaxies like NGC 1097 or NGC 7469. This result does not necessarily mean the nonexistence of an AGN in the center of these galaxies. The soft X-rays coming could be blocked very efficiently by the high molecular content in the luminous infrared galaxies. For example, the nuclear molecular gas density in Arp 220 is about 10 and 100 times larger than that measured in NGC 7469 and NGC 1097, respectively (Planesas, Colina, & Pérez-Olea 1996, and references therein).

5. CONCLUSIONS

High-resolution X-ray images of the composite AGN plus circumnuclear star-forming galaxies NGC 1097 and NGC 7469 have been presented. An extended X-ray emission is detected in the HRI image of NGC 1097. This emission is associated with the circumnuclear star-forming ring of this galaxy and accounts for 20% of its total X-ray luminosity. The integrated X-ray luminosity of NGC 1097 is $L_X = 2 \times 10^{41}$ ergs s^{-1}, a factor of 10 larger than that of previously detected LINERs and within the luminosity range of Seyfert 2 and low luminosity Seyfert 1 galaxies.

Circumnuclear star-forming rings in NGC 1097 and NGC 1068 are characterized by X-ray luminosities and $L_X/L_{5\ GHz}$ and $L_X/L_{H\alpha}$ ratios similar to those measured in nearby prototype starbursts like M82, NGC 253, and NGC 1808. On average, starbursts and circumnuclear star-forming rings are characterized by $L_X/L_{5\ GHz} \sim 400$, and $L_X/L_{H\alpha} \sim 0.14$.

In NGC 7469, the X-ray emission coming from the circumnuclear ring cannot be disentangled from that of the nucleus. However, assuming the starburst in NGC 7469 radiates with the average $L_X/L_{5\ GHz} \sim 400$ of starbursts, an X-ray luminosity $L_X = 5.6 \times 10^{41}$ ergs s^{-1} is inferred.

Circumnuclear star-forming rings in low- and intermediate-luminosity active galaxies like NGC 1097 and NGC 1068 account for 10%–20% of the total 0.1–2.4 keV X-ray luminosity emitted by these galaxies. In the high-luminosity Seyfert 1 NGC 7469, in which a circumnuclear star-forming ring dominates the bolometric energy output, the ring contributes only 4% of the total soft X-ray luminosity.

Pure AGNs are well differentiated from pure starbursts in the $L_X/L_{H\alpha}$ ratio. For a given Hα luminosity, pure AGNs are 100 times more luminous in X-rays than pure starbursts.

Weak X-ray sources detected in some ultraluminous infrared galaxies like NGC 3690 and Arp 220 are characterized by an X-ray to Hα and radio luminosity ratios $L_X/L_{H\alpha} \sim 0.05$ and $L_X/L_{5\ GHz} \sim 20$. These ratios are consistent with those measured in nearly edge-on starbursts like M82 and NGC 253 and about 100 times smaller than the ratios observed in standard AGN plus star-forming ring galaxies like NGC 1097 and NGC 7469.

D. P. O. wishes to thank Ed Colbert and Miguel Cerviño for useful discussions. D. P. O. acknowledges the support by the Spanish Council for Research and Technology (DGYCIT) under grant PB93-0252 and partial support by the Space Telescope Science Institute under grant DDRF-82090.

REFERENCES

Bi, H. G., Arp, H., & Zimmermann, H. U. 1994, A&A, 282, 386
Bland-Hawtorn, J., Sokolowsky, J., & Cecil, G. 1991, ApJ, 375, 78
Bohlin, R. C., Savage, B. D., & Drake, J. F. 1978, ApJ, 224, 132
Brandt, W. N., Fabian, A. C., Nandra, K., & Tsuruta, S. 1993, MNRAS, 265, 996
Bregman, J. N., & Pildis, R. A. 1992, ApJ, 398, L107
Bruhweiler, F. C., Truong, K. G., & Altner, B. 1991, ApJ, 379, 596
Colbert, E., Petre, R., Schlegel, E. M., & Ryder, S. D. 1995, ApJ, 446, 177
Colina, L., & Pérez-Olea, D. E. 1992, MNRAS, 259, 709
———. 1995, MNRAS, 277, 845
Condon, J. J., Condon, M. A., Gisler, G., & Puschell, J. J. 1982, ApJ, 252, 102
Condon, J. J., Huang, Z.-P., Yin, Q. F., & Thuan, T. X. 1991, ApJ, 378, 65
Dahlem, M., Hartner, G. D., & Junkes, N. 1994, ApJ, 432, 598
David, L. P., Harnden, F. R., Jr., Kearns, K. E., & Zombeck, M. V. 1995, The ROSAT High-Resolution Imager (HRI) (US *ROSAT* Science Data Center/SAO Tech. Rep.)
David, L. P., Jones, C., & Forman, W. 1992, ApJ, 388, 82
Doherty, R. M., Puxley, P. J., Lumsden, S. L., & Doyon, R. 1995, MNRAS, 277, 577
Eales, S. A., & Arnaud, K. A. 1988, ApJ, 324, 193
Elvis, M., Lockman, F. J., & Wilkes, B. J. 1989, AJ, 97, 777
Fabbiano, G. 1988a, ApJ, 325, 544
———. 1988b, ApJ, 330, 672
Fabbiano, G., Kim, D.-W., & Trinchieri, G. 1992, ApJS, 80, 531
Fabbiano, G., & Trinchieri, G. 1984, ApJ, 286, 491
———. 1987, ApJ, 315, 46
Filippenko, A. V., & Sargent, W. L. W. 1988, ApJ, 324, 134
Forbes, D. A., & Ward, M. J. 1993, ApJ, 416, 150
Forbes, D. A., Ward, M. J., Rotaciuc, V., Blietz, M., Genzel, R., Drapatz, S., van der Werf, P. P., & Krabbe, A. 1993, ApJ, 406, L11
Genzel, R., Weitzel, L., Tacconi-Garman, E., Blietz, M., Cameron, M., Krabbe, A., & Lutz, D. 1995, ApJ, 444, 129
Goldader, J. D., Joseph, R. D., Doyon, R., & Sanders, D. B. 1995, ApJ, 444, 97
Heckman, T. M., Armus, L., & Miley, G. 1990, ApJS, 74, 833
Heckman, T. M., Dahlem, M., Eales, S. A., Fabbiano, G., & Weaver, K. 1996, ApJ, 457, 616
Ho, P. T. P., Beck, S. C., & Turner, J. L. 1990, ApJ, 349, 57
Hummel, E. 1985, A&AS, 60, 293
Hummel, E., van der Hulst, J. M., & Keel, W. C. 1987, A&A, 172, 32 (HHK87)
Junkes, N., Zinnecker, H., Hensler, G., Dahlem, M., & Pietsch, W. 1995, A&A, 294, 2
Keel, W. C. 1983, ApJ, 269, 466
Kim, D.-W. 1989, ApJ, 346, 653
Kim, D.-W., Fabbiano, G., & Trinchieri, G. 1992, ApJS, 80, 645
Koratkar, A., Deutstua, S. E., Heckman, T., Filippenko, A. V., Ho, L. C., & Rao, M. 1995, ApJ, 440, 132
Krabbe, A., & Colina, L. 1996, ApJ, submitted
Krabbe, A., Sternberg, A., & Genzel, R. 1994, ApJ, 425, 72
Mas-Hesse, J. M., Rodríguez-Pascual, P. M., Sanz Fernández de Córdoba, L., & Mirabel, I. F. 1994, ApJS, 92, 599
Mauder, W., Weigelt, G., Appenzeller, I., & Wagner, S. J. 1994, A&A, 285, 44
Meixner, M., Puchalski, R., Blitz, L., Wright, M. C. H., & Heckman, T. M. 1990, ApJ, 354, 158
Miller, J. S., & Goodrich, R. W. 1990, ApJ, 355, 456
Morse, J. A. 1994, in The Soft X-Ray Cosmos, ed. E. M. Schlegel & R. Petre (New York: AIP), 258
Morse, J. A., Wilson, A. S., Elvis, M., & Weaver, K. 1995, ApJ, 439, 121
Neff, S. A., Fanelli, M. N., Roberts, L. J., O'Connell, R. W., Bohlin, R., Roberts, M. S., Smith, A. M., & Stecher, T. P. 1994, ApJ, 430, 545
Niklas, S., Klein, U., & Wielebinski, R. 1995, A&A, 293, 56
Petre, R., Mushotzky, R. F., Serlemitsos, P. J., Jahoda, K., & Marshall, F. E. 1993, ApJ, 418, 644
Phillips, M. M., Pagel, B. E., Edmunds, M. G., & Díaz, A. 1984, MNRAS, 210, 701
Pietsch, W., Vogler, A., Kahabka, P., Jain, A., & Klein, U. 1994, A&A, 284, 386
Planesas, P., Colina, L., & Pérez-Olea, D. E. 1996, A&A, submitted
Rieke, G. H. 1988, ApJ, 331, L5
Rotaciuc, V., Krabbe, A., Cameron, M., Drapatz, S., Genzel, G., Sternberg, A., & Storey, J. W. V. 1991, ApJ, 370, L23
Ryder, S. D., Stavely-Smith, L., Dopita, M. A., Petre, R., Colbert, E., Malin, D., & Schlegel, E. M. 1993, ApJ, 416, 167
Saikia, D. J., Unger, S. W., Pedlar, A., Yates, G. J., Axon, D. J., Wolstencroft, R. D., Taylor, K., & Gyldenkerne, K. 1990, MNRAS, 245, 397
Schlegel, E. M. 1994, in The Soft X-Ray Cosmos, ed. E. M. Schlegel & R. Petre (New York: AIP), 195
Schuder, J. M. 1980, ApJ, 240, 32
Schulz, H., Knake, A., & Schmidt-Kaler, Th. 1994, A&A, 288, 425
Storchi-Bergmann, T., Baldwin, J. A., & Wilson, A. S. 1993, ApJ, 410, L11
Storchi-Bergmann, T., Eracleous, M., Livio, M., Wilson, A. S., Filippenko, A. V., & Halpern, J. P. 1995, ApJ, 443, 617
Turner, T. J., George, I. M., & Mushotzky, R. F. 1993, ApJ, 412, 72
Turner, T. J., & Ho, P. T. P. 1994, ApJ, 421, 122
Ulvestad, J. S., & Wilson, A. S. 1984a, ApJ, 278, 544
———. 1984b, ApJ, 285, 439
———. 1989, ApJ, 343, 659
Veilleux, S., Kim, D.-C., Sanders, D. B., Mazzarella, J. M., & Soifer, B. T. 1995, ApJS, 98, 171
Ward, M. J. 1988, MNRAS, 231, 1P
Watson, M. G., Stanger, V., & Griffiths, R. E. 1984, ApJ, 286, 144
Weaver, K. A., Mushotzky, R. F., Serlemitsos, P. J., Wilson, A. S., Elvis, D., & Briel, U. 1995, ApJ, 442, 597
Wilson, A. S., Baldwin, J. A., Sun, S. D., & Wright, A. E. 1986, ApJ, 310, 121
Wilson, A. S., Elvis, M., Lawrence, A., & Bland-Hawthorn, J. 1992, ApJ, 391, L75
Wilson, A. S., Helfer, T. T., Haniff, C. A., & Ward, M. J. 1991, ApJ, 381, 79
Wrobel, J. M. 1991, AJ, 101, 127